

Lformer: Text-to-Image Generation with L-shape Block Parallel Decoding

Jiacheng Li¹, Longhui Wei^{2,3}, ZongYuan Zhan², Xin He², Siliang Tang¹, Qi Tian², Yueting Zhuang¹
¹Zhejiang University ²Huawei Cloud ³University of Science and Technology of China

{jiachengli, siliang, yzhuang}@zju.edu.cn, weilh2568@gmail.com

{zhanzongyuan, hexin80, tian.qil}@huawei.com

Abstract

Generative transformers have shown their superiority in synthesizing high-fidelity and high-resolution images, such as good diversity and training stability. However, they suffer from the problem of slow generation since they need to generate a long token sequence autoregressively. To better accelerate the generative transformers while keeping good generation quality, we propose Lformer, a semi-autoregressive text-to-image generation model. Lformer firstly encodes an image into $h \times h$ discrete tokens, then divides these tokens into h mirrored L-shape blocks from the top left to the bottom right and decodes the tokens in a block parallelly in each step. Lformer predicts the area adjacent to the previous context like autoregressive models thus it is more stable while accelerating. By leveraging the 2D structure of image tokens, Lformer achieves faster speed than the existing transformer-based methods while keeping good generation quality. Moreover, the pretrained Lformer can edit images without the requirement for finetuning. We can roll back to the early steps for regeneration or edit the image with a bounding box and a text prompt.

1. Introduction

Recent years have seen significant progress in the task of text-to-image (T2I) generation. The fidelity, diversity, and text relevance of the synthesized images are greatly improved with large-scale models [45, 35] and datasets [39, 40]. Generative transformers¹ [32, 7, 13, 48, 22, 52, 11, 8, 16] are one of the popular generative methods receiving growing interest. Generally, they consist of two stages: Firstly, it uses a Vector Quantized Variational AutoEncoder (VQ-VAE) [44] to compress an image into discrete image tokens, which can be decoded back into an image at inference time; Secondly, it learns to generate image

¹The early works of this approach are autoregressive models, whose name is better known by the community. But there are non-autoregressive models and discrete diffusion models later, so we call them ‘generative transformers’ appropriately.



Figure 1: Selected 256×256 samples generated by our model. Lformer can generate both photorealistic and artistic content.

tokens from the text input with a transformer model. The transformer architecture is flexible for scaling up, and the maximum likelihood estimation (MLE) ensures better training stability and diversity compared with previous GAN-based models [50, 55, 42].

Despite the success these methods have achieved, they still suffer from the slow generation problem. Most of the existing generative transformers [32, 7, 48, 13, 52] leverage autoregressive (AR) models, which rearrange the 2D image tokens in the raster-scan order and decode only one token in each step. Therefore, they take 1024 forward steps with a large-scale transformer to generate 32×32 tokens for a single 256×256 image, which consumes about 30 seconds on a V100 GPU. However, the users have a high requirement for generation speed, since they usually need to generate dozens of candidates to obtain the image they expect.

Some recent works [2, 54, 8, 16] can generate 32×32 tokens within a few steps with the design of parallel de-

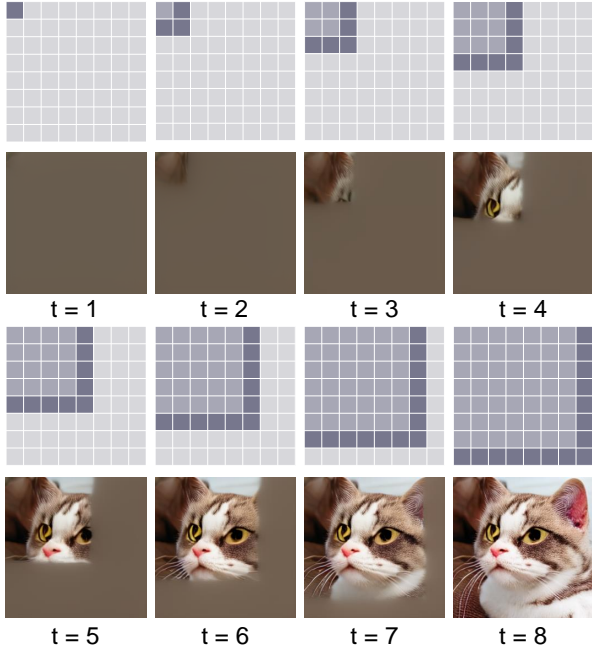


Figure 2: Generation process of Lformer (taking $h \times w = 8 \times 8$ as an example). We divide an image token map into h mirrored L-shape blocks from the top left to the bottom right. At each step, we generate all the tokens in an L-shape block parallelly.

coding strategy like Mask-Predict [14]) and Discrete Diffusion (DD) [16, 20], which has greatly improved the inference speed. However, the speed of a transformer depends not only on the number of decoding steps but also on the forward time of each step, which is quadratic with the sequence length. The existing methods [14, 54, 8, 2] forward with full $h \times w$ tokens in every step. Thus there is still much room for the optimization of the inference time at each step.

To better accelerate the generative transformers while keeping good generation quality, we propose Lformer, a semi-autoregressive (SAR) T2I generation model that parallelly decodes image tokens in L-shape blocks, which can generate high-quality images at a high speed. Lformer is fast because it generates images within a small number of steps and processes only partial tokens in each step. Specifically, as shown in Fig. 2, we generate image tokens in a $h \times h$ window and divide these tokens into h mirrored L-shape blocks from the top left to the bottom right. At each step, we generate the tokens in a block parallelly. The newly generated tokens expand the context to a larger square, and we finish the generation in h steps.

Lformer achieves parallelism by leveraging the 2D structure of image tokens. Thus it can keep good generation quality while greatly improving the sampling speed. The area predicted by Lformer in each step is adjacent to the

square context. Such adjacent areas have a stronger association with the context than the non-adjacent area, which will make the operation of predicting them easier. The process of extending adjacent tokens is similar to the process of autoregressive models and our model can benefit from the techniques of unidirectional models, such as teacher forcing [47] for efficient training and attention cache [51] for fast inference. Note that only Lformer achieves such compatibility between parallelism and unidirectional techniques in T2I generation due to its semi-autoregressive design, whereas NAR methods can not leverage the techniques like attention cache.

Additionally, the pretrained Lformer has the potential capability to edit images without the requirement for additional fine-tuning. This is because the discrete tokens have strong space mapping relations with the generated images, and our generation process is trackable. So when encountering a local defect, we can roll back to the early steps for regeneration or edit the image with a bounding box and a text prompt, as shown in Section 5.5.

We train our model on three T2I datasets of different scales: Multi-Modal CelebA-HQ [49] containing 30K face images, CC3M [40] and a subset of LAION [39] respectively containing 3M and 90M general domain images for large-scale training. Compared with the existing transformer-based methods, our method is much faster while achieving even better a Fréchet Inception Distance (FID)[17] score on MMCelebA-HQ. Lformer also shows competitive performance on MS-COCO 2014 in both zero-shot and fine-tuning settings. Moreover, our pretrained model can even generate counterfactual images with good quality, as shown in Fig. 2.

2. Related Work

2.1. Text-to-Image Generation

The task of text-to-image (T2I) generation aims to synthesize images from the given text descriptions. The early deep-learning-based T2I models like AttnGAN [50], DM-GAN [55], DF-GAN [42] build upon Conditional Generative Adversarial Nets (CGAN) [25]. These models can generate high-quality images for specific domains like birds [46] and flowers [27], but the general-domain generation presents great challenges for them. Later, a series of works [33, 32, 7, 48, 13, 22, 52, 11] adopt a two-stage framework that leverages an image tokenizer to compress an image to a sequence of discrete tokens and treat the T2I generation as a sequence-to-sequence modeling problem. They train a large-scale transformer[45] with a hundreds-million-scale dataset and achieve great advancement on the general-domain generation. Recently, diffusion models like GLIDE [26], DALL-E 2 [31], Imagen [36], LDM [34] also show great effectiveness on general-domain T2I generation.

2.2. Autoregressive Models for T2I

The early works of Autoregressive (AR) Models [43, 38, 4, 3] directly generate at the pixel level, whose resolution is limited by heavy computation. Later works like DALL-E [32] and Cogview [7] compress an image with VQ-VAE [44] and model the text and image tokens with a transformer. Esser *et al.* propose VQGAN [12], an image tokenizer that can reconstruct images with better photorealism. NÜWA [48] proposes a 3D transformer encoder-decoder framework to further leverage videos. Make-A-Scene [13] introduces additional controlling elements, such as the segmentation map. Parti [52] scale the transformer up to 20B parameters, achieving an impressive zero-shot FID score [17] of 7.23 on MS-COCO 2014 [24].

2.3. Parallel Decoding Models for T2I

The current transformer-based T2I models that can achieve parallel decoding are mainly non-autoregressive (NAR) Models. They usually achieve faster inference speed than autoregressive models while keeping similar generation quality. Some existing NAR methods [2, 8] for T2I are inspired by the works of natural language generation (Mask-Predict [14], GLAT [28], GLM [10]). UFC-BERT [54] and MaskGIT [2] adopt the bidirectional mask-and-predict framework like BERT [6] and Mask-Predict [14]. The key idea of these methods is to predict all tokens simultaneously in parallel but only replace the mask tokens that get the highest confidence in each step. As for other NAR methods, Cogview2 [8] combines autoregressive blank filling with hierarchical generation. There are also works like VQ-Diffusion [16] that leverage diffusion in the token space to achieve parallelism.

3. Method

3.1. Preliminaries

Most of autoregressive (AR) and non-autoregressive (NAR) methods are based on two-stage image generation frameworks [12, 32, 7], and the key difference between them lies in the decoding process in the second stage. Lformer is also carefully designed for a more efficient decoding scheme. Therefore, before introducing the details of Lformer, we first review the general framework of two-stage image generation methods.

In the first stage, the algorithm learns an encoder E, a decoder D, and a codebook $e = \{e_k\}_{k=1}^K \subset \mathbb{R}^{n_e}$, where n_e is the dimensionality of codes, K is the size of codebook. They work together to compress an image $x \in \mathbb{R}^{H \times W \times 3}$ into discrete tokens $s = \{s_i\}_{i=1}^N, s_i \in \{0, \dots, |e| - 1\}$ and reconstruct the image with these tokens. Specifically, the encoder E encodes an image into spatial codes $\hat{e} = E(x) \in \mathbb{R}^{h \times w \times n_e}, h = H/f, w = W/f, f = 2^m$, where f is

the downsampling factor, m is the number of downsampling blocks in the encoder E. This $h \times w \times n_e$ tensor can be viewed as $h \times w$ codes of $\hat{e}_{ij} \in \mathbb{R}^{n_e}$, where i, j denote the code indices in $h \times w$. Each spatial code \hat{e}_{ij} in \hat{e} is quantized by replacing it with its nearest prototype vector in the codebook:

$$\mathbf{q}(\hat{e}_{ij}) = e_k, \text{ where } k = \arg \min_k \|\hat{e}_{ij} - e_k\| \quad (1)$$

where \mathbf{q} denotes the quantization operation. We can reconstruct the image from the quantized codes $\tilde{e} = \mathbf{q}(\hat{e}) \in \mathbb{R}^{h \times w \times n_e}$ by:

$$\hat{x} = D(\tilde{e}) = D(\mathbf{q}(E(x))) \quad (2)$$

The above process is supervised by reconstruction loss [44, 33], optionally with perceptual loss [9, 12] and GAN loss [12]. The quantized codes \tilde{e} can be further represented by their indices in the codebook, which we call image tokens:

$$s = \{s_{ij}\} \in \{1, \dots, K\}^{h \times w} \quad (3)$$

$$s_{ij} = k \text{ such that } \tilde{e}_{ij} = e_k$$

By mapping the image tokens s back to their corresponding codebook entries, we can recover the quantized codes \tilde{e} and further decode it to an image by $\hat{x} = D(\tilde{e})$.

In the second stage, the key is to learn the prior $p(s|c)$ generation model, where c denotes the condition. Take AR methods as example, they generally rearrange $s^{h \times w}$ into raster-scan order $s^{h \cdot w}$ and predict one token at each step:

$$p(s|c) = \prod_{t=1}^{h \cdot w} p(s_t | s_{[1:t-1]}, c) \quad (4)$$

where $s_{[1:t-1]}$ denotes $\{s_1, s_2, \dots, s_{t-1}\}$. Once a sequence s is sampled, we can obtain the corresponding generated image by decoding s with the decoder D.

3.2. L-shape Parallel Decoding

Although AR and NAR methods have achieved great success, the AR methods suffer from low generation speed when achieving high generation quality, and the NAR methods suffer from unstable generation quality when achieving high generation speed. In order to accelerate the generative transformers while keeping good generation quality, we propose a semi-autoregressive decoding strategy, L-shape Parallel Decoding. It can parallelly decode tokens in a step while considering the unidirectional characteristic of AR models by leveraging the 2D structure of image tokens. Specifically, we generate square images (e.g. 256×256), and we have $h = w$ for image tokens. We divide $h \times h$ image tokens into h blocks from the top left to the bottom right, with each block in a mirrored L-shape (the first block

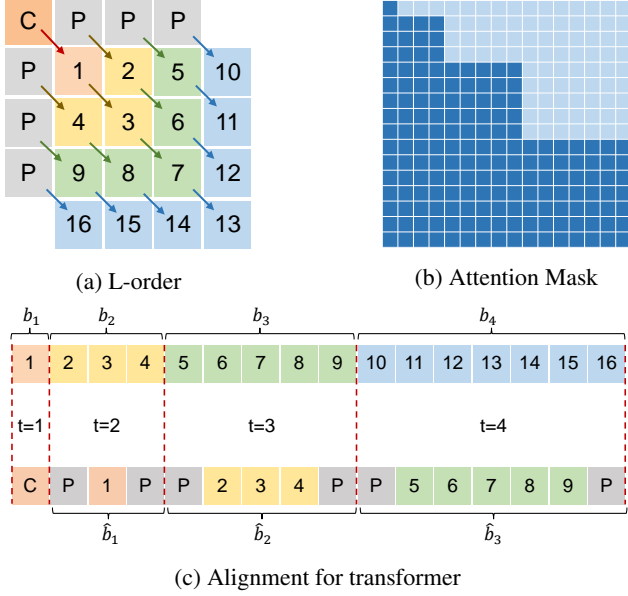


Figure 3: L-shape Parallel Decoding. (a) We rearrange the tokens in L-order and generate the tokens in an L-shape Block (marked in colors) in a step parallelly. C denotes the condition, and P denotes a pad token. (b) Causal attention mask for the transformer implementation of Lformer. The tokens in a block can attend to the context of previously generated tokens which forms a square. (c) We add pad tokens at both sides of the previous L-block to align with the next L-block for transformer implementation.

only has the single top left token as a special case) numbered from 1 to h . As shown in Fig. 3a, we rearrange the tokens in the order that considers the block order first and iterate clockwise within a block. So the t -th L-block will contain tokens of $s_{[(t-1)^2+1:t^2]}$ and the context of previous t steps is a square $s_{[1:(t-1)^2]}$. We decode $h \times h$ tokens in h steps and parallelly decode all the tokens in the t -th block at time step t , with $t = 1, \dots, h$:

$$p(s|c) = p(s_1|c) \cdot \prod_{t=2}^h p(s_{[(t-1)^2+1:t^2]}|s_{[1:(t-1)^2]}, c) \quad (5)$$

where $p(s_1|c)$ means we directly generate the token s_1 from the condition c for $t = 1$. For clarity and simplicity, we denote the t -th L-block $s_{[(t-1)^2+1:t^2]}$ as b_t , and the square context $s_{[1:t^2]}$ as $s_{<t^2}$ in the rest of this paper.

To implement Eq. (5) with a transformer-based generation model, we need to fill the sequence with pad tokens for alignment, since the output length for a transformer is the same as its input length. Each L-block b_t contains $2t - 1$ tokens, and the number of tokens contained in adjacent blocks differs by two. So we insert pad tokens at both sides of the $(t - 1)$ -th L-block b_{t-1} to align with the t -th L-block b_t , as

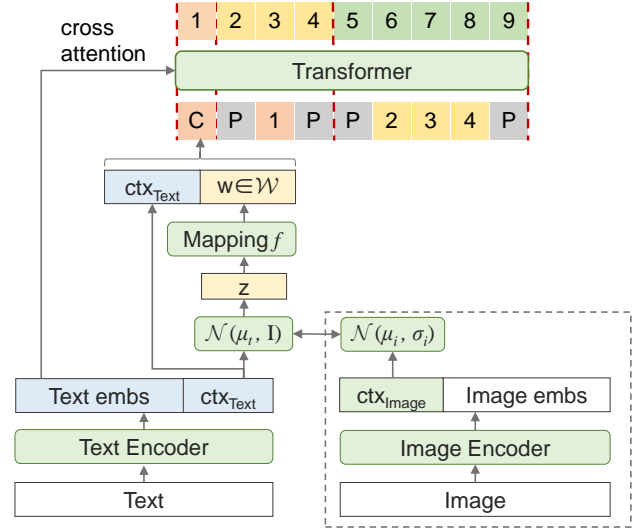


Figure 4: Model structure of Lformer. We adopt CVAE to introduce a latent variable w for global representation to the inconsistency of parallel generation. We concatenate w to the global text feature as the final condition. The part in the dashed box is removed at inference time.

shown in Fig. 3c. The alignment for the transformer can be formulated as:

$$\hat{b}_t = \text{pad}(b_t) = [\text{P}; b_t; \text{P}] \quad (6)$$

$$[b'_1; b'_2; \dots; b'_t] = \text{Transformer}([c; \hat{b}_1; \hat{b}_2; \dots; \hat{b}_{t-1}]) \quad (7)$$

where b_t is the t -th L-block of ground truth tokens, P denotes a pad token, $[\cdot]$ denotes the concatenation, \hat{b}_t denotes the padded b_t . The model's output at the place corresponding to the \hat{b}_{t-1} will be used to predict b_t , and we denote the model's prediction for b_t as b'_t . We train the model with the average cross-entropy [12, 52] of all $h \times h$ tokens: $L = \frac{1}{h^2} \sum_{t=1}^h \text{CE}(b'_t, b_t)$, where CE denotes the sum of the cross-entropy of tokens in b'_t and b_t .

With such a design, we can train Lformer in the way of teacher-forcing [47] with a causal attention mask shown in Fig. 3b. This is efficient for training since all the tokens contribute to the cross-entropy loss. Besides, at inference time, we can further accelerate with the attention cache mechanism [51], by which we cache the keys and values of previous steps to avoid redundant calculations.

3.3. Global Representation for Parallel Decoding

Since Lformer decodes the $2t - 1$ tokens in the L-block parallelly, the probabilities of tokens in the same block are independent, which will make the model partially exhibit *conditional independence* (discussed in Sec 2.3 of [15], the multimodality problem of parallel decoding). To preserve the stability of the generation process, an extra global rep-

resentation for the constraint is required in Lformer. Similar to [1, 19], we adopt the Conditional Variational Auto-Encoder (CVAE) [41] to enhance the generation consistency. Fig. 4 shows the model structure of Lformer. We use CLIP [29] text encoder to extract text features, treat the CLIP image encoder ϕ as the encoder of CVAE, and treat the transformer model θ as the decoder of CVAE, then we have:

$$\mathcal{L}_{\text{CVAE}}(x, \hat{c}; \theta, \phi) = -\text{KL}(q_\phi(z|x, \hat{c})||p_\theta(z|\hat{c})) + \mathbb{E}_{q_\phi(z|x, \hat{c})}(\log p_\theta(x|z, \hat{c})) \quad (8)$$

where x is an image sample, \hat{c} is the text context embedding extracted by CLIP text encoder, KL denotes Kullback-Leibler (KL) Divergence, $q_\phi(z|x, \hat{c})$ is a Gaussian distribution $\mathcal{N}(\mu_i, \sigma_i)$ estimated by the CLIP image encoder ϕ , $p_\theta(z|\hat{c})$ is a Gaussian distribution $\mathcal{N}(\mu_t, I)$ estimated by the CLIP text encoder. The condition c for the transformer input is:

$$c = [\hat{c}; f(z)] \quad (9)$$

where $f(\cdot)$ is a mapping function consisting of fully connected layers that map the Gaussian latent variable z to the \mathcal{W} space [21].

In the framework of CVAE, we estimate a Gaussian distribution for each image and constraint this distribution to the distribution estimated by its corresponding text with KL Divergence. With such a design, we can sample a latent variable z from $p_\theta(z|\hat{c})$ as the representation of the image instance we sample for the given text \hat{c} . The second term of Eq. (8) is the reconstruction loss, which we can estimate by Eq. (5) with cross-entropy since we have $x = D(s)$.

Note that we do not need the CLIP image encoder ϕ (the part in the dashed box) at inference time since we can sample z from $p_\theta(z|\hat{c})$. Our final model consists of a transformer, a mapping function f , and a CLIP text encoder. We also use cross-attention to enhance the text semantics.

4. Computation Complexity Analysis

Lformer is faster not only for a small number of decoding steps but also for its context structure. The computation complexity of a transformer mainly comes from the attention mechanism [45]. We denote the length of the context as N ($h \times h$, usually 256 or 1024), the hidden dimension as D , and the inference steps as T . The computation in the attention mainly comes from the matrix multiplication of $Q \cdot K^T \cdot V$, where $Q, K, V \in \mathbb{R}^{N \times D}$. The total number of multiplications of a bidirectional model (e.g., the BERT model used in NAR methods) is proportional to TN^2D . As for Lformer, while working with the attention cache, we have $Q \in \mathbb{R}^{(2t-1) \times D}$ and $K, V \in \mathbb{R}^{t^2 \times D}$. Thus the number of multiplication operations is

$$M = \sum_{t=1}^{\sqrt{N}} (2t-1)t^2D = \left(\frac{1}{2}N^2 + \frac{2}{3}N^{\frac{3}{2}} - \frac{1}{6}\sqrt{N}\right)D \quad (10)$$

When we have $N=1024$, $T=\sqrt{N}$, $D=1024$, the number of attention multiplication M for a bidirectional model is 33B whereas Lformer gets its M of 0.5B, which is much smaller.

5. Experiments

5.1. Experimental Setup

Datasets We train Lformer on three datasets with different scales: Multi-Modal CelebA-HQ [49] (MMCelebA-HQ) containing 30 thousand samples, Conceptual Captions (CC3M) [40] containing 3 million samples, and a subset of LAION400M [39] containing 90 million images, which we call LAION90M.

Implementation Details We use CLIP-ViT-B/16 [29] as the text encoder and freeze the parameters during training. We generate 256×256 images for all datasets. To save GPU memory, we adopt techniques of the ZeRO optimization [30], block sparse attention [5], and activation checkpointing. All models are trained in float16 precision, and we adopt PB-relax and Sandwich LayerNorm proposed by [7] to keep stability. We use top- k [12, 7, 22] and top- p [18, 22] sampling during inference. The structures of the transformers vary by dataset, and we show their details in the corresponding sections. In the rest of the paper, we use L, H, and D to denote the number of layers, attention heads, and the hidden dimension of a transformer, respectively. More details about the datasets and implementation are available in the Appendix.

5.2. Comparison of Inference Speed

We first verify the speed of Lformer and compare it with the existing transformer-based methods in Table 1. We generate a batch of 32 images with 32×32 tokens, and the decoding time of the VQGAN is included in the ‘‘BatchTime’’. All the tests are done with the same machine with a V100 GPU, and we report the average time of 10 batches. We follow the setting of VQ-DIFFUSION [16] and test with a transformer of $L=19$, $H=16$, and $D=1024$ except for RQVAE [22]. RQVAE generates images with a token map of $8 \times 8 \times 4$, and it has an extra Depth Transformer. Thus we separately compare an RQVAE of $L=26+4$ (4 layers for Depth Transformer.), $H=20$, $D=1280$, with an Lformer of $L=30$, $H=20$, $D=1280$ by generating 16×16 tokens. VQ-Diffusion [16] can generate in 25 to 100 steps, and we test it with 32 steps for a fair comparison.

As shown in Table 1, Lformer achieves the fastest inference speed of 3.57s for a batch when working with the attention cache [51]. It also surpasses RQVAE [22] with 2.37s on the 16×16 tokens generation. Note that only the unidirectional models like AR and Lformer can leverage attention cache. We also find that the AR model (Our implemented version of AR uses cross-attention) is surprisingly fast with the attention cache. This is because the early steps

Methods	Steps	Params	Batch Time(s)	s/img	img/s
AR [12]	1024	322M	1270.0	39.7	0.025
AR-cache [12]	1024	322M	33.94	1.06	0.942
VQ-Diffusion [16]	32	370M	86.02	2.67	0.372
MASKGIT [2]	8	322M	21.05	0.672	1.49
Lformer (Ours)	32	322M	26.0	0.813	1.23
Lformer-cache (Ours)	32	322M	3.57	0.112	8.96
RQVAE [22]	256	654M	5.32	0.166	6.02
Lformer-cache (Ours)	16	798M	2.37	0.074	13.5

Table 1: Speed comparison. We compare to the existing transformer-based methods with the same structure of L=19, H=16, and D=1024. We generate a batch of 32 images with 32×32 tokens except for RQVAE [22]. We separately compare with RQVAE using a fair setting. Note that only unidirectional models like AR and Lformer can leverage attention cache.

Model	Type	Params	FID↓	s/img↓
VQGAN* [12]	AR	406M	19.52	3.676
UFC-BERT* [54]	NAR	406M	23.62	0.168
LPD	SAR	406M	20.93	0.046
UFC-BERT+CVAE*	NAR	406M	22.65	0.168
LPD+CVAE	SAR	406M	19.91	0.046
Lformer-S	SAR	102M	23.30	0.030
Lformer-M	SAR	229M	22.13	0.036
Lformer-L	SAR	406M	19.91	0.046
Lformer-E	SAR	1B	18.60	0.076

Table 2: Comparison on MMCelebA-HQ. We test the effect of decoding strategies, CVAE module, and model scales. LPD+CVAE is equivalent to Lformer-L. * denotes our implementation.

of a unidirectional model have a partial context ($< h \times h$ tokens) while a NAR model forwards with a full context ($h \times h$ tokens) at each step.

5.3. Comparison on MMCelebA-HQ

After verifying the efficiency of Lformer, we further test its generation quality on MMCelebA-HQ [49]. Following UFC-BERT [54], we set the transformer structure to L=24, H=16, and D=1024 and generate in the latent of 16×16 tokens. As shown in Fig. 5, Lformer can generate high-quality images with the text prompts from the MMCelebA-HQ dataset. To demonstrate the effectiveness and scalability of our method, we further compare models with different decoding strategies, module settings, and model scales by their Fréchet Inception Distance (FID)[17] scores and generation speed. The implementation details of these models are available in the Appendix.



Figure 5: Random samples of 256×256 generated by Lformer-L with the text prompts from the MMCelebA-HQ validation set.

Strategy Comparison. We compare models with decoding strategies of the standard autoregressive (AR) scheme (e.g., VQGAN [12]), the mask and predict (NAR) scheme (e.g., UFC-BERT [54]), and our L-shape Parallel Decoding (LPD). During the comparison, we do not use any global representation and use the same first-stage model and transformer model. As shown in Table 2, the AR method has better generation quality but generates slowly, and the NAR method shows a great improvement in generation speed but obtains a higher FID score of 23.62. By comparison, our LPD obtains a lower FID score of 20.93 with a much faster speed of 0.046 s/img. This shows that Lformer can keep good generation quality with a high inference speed since it leverages the prior of the 2D structure of images.

Module Effect. We compare the model with and without the global representation provided by CVAE to show its effect. We also apply it to the NAR method like UFC-BERT which also uses parallel decoding. Note that LPD+CVAE is equivalent to the full model Lformer-L. The model with the global representation achieves a lower FID score of 19.91 because the global representation relieves the conditional independence problem in parallel decoding.

Scalability. Generally, the performance is gradually improved as the model size grows. Besides, we also observe quality improvement when scaling the model from 229M to 406M. The phenomenon of quality improvement is also observed in Parti[52].

5.4. Comparison on MS-COCO

The current text-to-image research [7, 8, 13, 32, 52, 53] mainly evaluates their models on MS-COCO 2014, where they pretrain a model on a large-scale dataset and then measure both zero-shot and fine-tuned generation quality on MS-COCO. We follow this setting and train Lformer models on CC3M and LAION90M, respectively. To fit such large datasets, we also scale up the model to 1B parameters with the transformer structure of L=24, H=16, and D=1536.

Models	Zero-shot			Finetuned				
	FID↓	IS↑	CLIPSIM↑	FID↓	Type	Params	Data	Computation
VQ-Diffusion* [16]	32.8*	15.2*	0.2539*	-	DD	0.5B	12M	-
DALL-E [32]	27.5	17.9	-	-	AR	12B	250M	430K×6K
Cogview [7]	27.1	18.2	0.3325	-	AR	4B	30M	144K×6K
RQVAE [22]	16.9	23.76*	0.3058*	-	AR	3.9B	30M	-
NÜWA [48]	-	-	-	12.9	AR	0.87B	2.9M+Video	50M×128
CogView2 [8]	24.0	22.4	-	17.4	NAR	6B	30M	300K×4K
Lformer-E (CC3M)	24.11	19.78	0.3052	-	SAR	1B	2.5M	240K×1K
Lformer-E (LAION90M)	15.01	26.22	0.3289	9.57	SAR	1B	90M	300K×1K
ERNIE-ViLG [53]	14.7	-	-	7.9	AR	10B	145M	-
Make-A-Scene [13]	11.84	-	-	7.55	AR	4B	35M+SEG	170K×1K
Parti [52]	7.23	-	-	3.2	AR	20B	1.8B+4B	450K×8K

Table 3: Performance comparison on MS-COCO 2014 [24]. Lformer samples 16 images per text prompt and reranks with a CLIP [29] model. * denotes the result that we evaluate with their released model (also rerank with 16 samples). ↓ denotes lower better and ↑ denotes higher better. The ‘Computation’ column shows the training cost in the form of ‘training steps × batch size’.

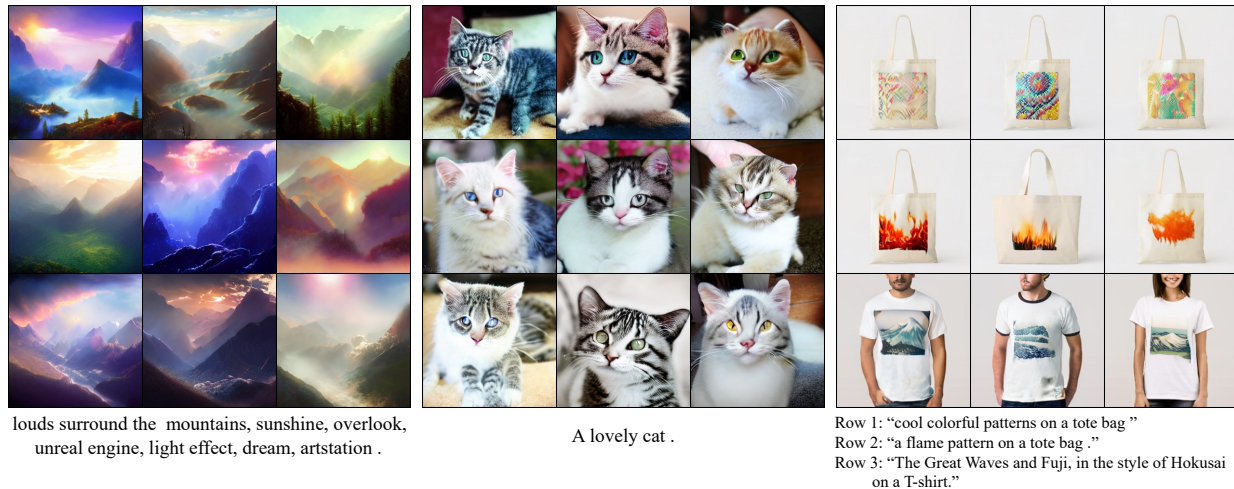


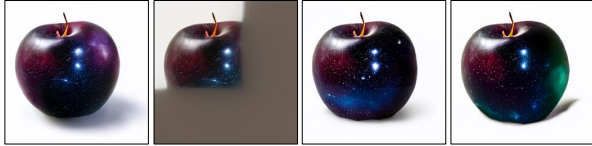
Figure 6: Diversity and composition capability. We show the images generated with the same text prompt. We also try the combination of a pattern and a carrier (tote bag or T-shirt) to show the creativity of the model.

We adopt the Transformer Classifier-Free Guidance (CFG) [13] with a scale of 3.0 and generate with 32×32 tokens. For each caption, we generate 16 images and select the best one with CLIP reranking score [32]. This model takes about 9 seconds (with CFG) to generate a batch of 16 images on a V100 GPU.

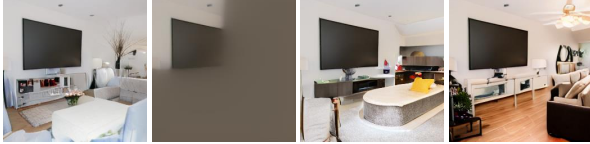
Following [32, 7, 52], we generate 30,000 images for the evaluation on MS-COCO [24]. We use metrics² of Fréchet Inception Distance (FID) [17], Inception Score (IS) [37] and CLIPSIM [48] to indicate the fidelity, diversity, and text-image relevance, respectively.

²We use the same evaluation code of prior works [32, 7] from <https://github.com/MinfengZhu/DM-GAN>

Quantitative Analysis Table 3 shows the performance comparison of Lformer and other generative transformer T2I models. The Lformer trained on LAION90M achieves an FID score of 15.01 and an IS of 26.22, which is competitive in transformer-based methods. Parti [52] demonstrates that the performance of the generative transformers can be significantly improved as the model scale grows. Thus the tens-billion-scale models are still leading in the FID score. Make-A-Scene [13] gets a lower FID score with the help of the segmentation maps thus we do not directly compare with it. We also find that the the scale of pre-training dataset plays an important role. The model trained on LAION90M [23] outperforms the model trained



Text input: *a black apple with cosmic texture in the white background.*



Text input: *a living room with a TV.*



Original text: *he has big nose , bags under eyes , mouth slightly open , high cheekbones , double chin , gray hair , and receding hairline .*
 Repaint text: *she is wearing heavy makeup . she wears lipstick.*

Figure 7: Repainting examples. We can generate variations for an image or achieve the effect of style mixing with different text prompts.

on CC3M by a large margin. Lformer has the potential to get better results if trained with more resources (both data and computation resources). Besides, we finetune Lformer on the MS-COCO [24] dataset and report the finetuned FID score. Lformer achieves a finetuned FID score of 9.57, which is better than the finetuned FID score of Cogview2 and NUWA.

Visual Analysis Lformer is capable of generating high-quality images with complex text inputs. As shown in Fig. 1, Lformer can generate both photorealistic and artistic content. Fig. 6 shows the diversity of the generated images. We also try the combination of a pattern and a carrier (tote bag and T-shirt) to show the creativity of the model.

5.5. Image Editing Applications

Lformer has the capability to edit images without the requirement of additional fine-tuning. The discrete tokens have strong space-mapping relations with the generated images. Thus we can edit an image by modifying the corresponding tokens of the target area. Based on this, we show two image editing applications: repainting and inpainting.

Repainting Given $h \times h$ tokens of an image, we can roll back to the early step t by keeping the early $t \times t$ tokens and regenerate the rest of the tokens. Fig. 7 shows examples of repainting. The first row and the second row show that we can generate variations of an image. In the third row, we generate an image with the description of a male and repaint it with the description of a female. The output image keeps some features of the original image and also introduces the



he is bald and has gray hair , and big nose .

he is wears eyeglasses.

he has mouth slightly open .

output



a painting of a cat

\emptyset

a painting of a cat wearing sunglasses

output



a cup of coffee

a cup of coffee

a cup of milk tea

output

Figure 8: Examples of conditional inpainting with a bounding box and a text prompt. We first generate an image with a text prompt and then repair defects, or edit the image with a different text prompt.

new features of the given text.

Inpainting Given a bounding box $(\hat{x}_1, \hat{y}_1, \hat{x}_2, \hat{y}_2)$ (coordinate of the top, left, bottom, and right), we map it to the corresponding region (x_1, y_1, x_2, y_2) in the token space by $x_1 = \lfloor \frac{\hat{x}_1}{f} \rfloor, y_1 = \lfloor \frac{\hat{y}_1}{f} \rfloor, x_2 = \lceil \frac{\hat{x}_2}{f} \rceil, y_2 = \lceil \frac{\hat{y}_2}{f} \rceil$, f is the downsampling factor. Then we regenerate the L-block containing this region, which is the block generated between the step of $[\max(x_1, y_1), \max(x_2, y_2)]$. We only replace the tokens in the box region and keep the rest tokens; This replacement is performed immediately in each inpainting step, instead of regenerating all L-blocks and then replacing them. Besides, Lformer also supports conditional inpainting with a different text input. Fig. 8 shows examples of inpainting. We can repair local defects or iteratively create an image by continuous inpainting.

5.6. Conclusion

In this paper, we propose Lformer, a semi-autoregressive text-to-image generation model that decodes image tokens in an L-shape block parallelly. Lformer achieves a faster speed than the existing transformer-based models while keeping a competitive performance. Lformer can also produce image variations and edit an image with a text prompt. Lformer currently generates images in a square window. Thus we consider leveraging the sliding window mechanism to generate non-square images in future work. We also consider higher resolution generation by decoding with more tokens or working with an extra upsampling model.

References

- [1] Samuel R. Bowman, Luke Vilnis, Oriol Vinyals, Andrew M. Dai, Rafal Józefowicz, and Samy Bengio. Generating sentences from a continuous space. In Yoav Goldberg and Stefan Riezler, editors, *Proceedings of the 20th SIGNLL Conference on Computational Natural Language Learning, CoNLL 2016, Berlin, Germany, August 11-12, 2016*, pages 10–21. ACL, 2016.
- [2] Huiwen Chang, Han Zhang, Lu Jiang, Ce Liu, and William T. Freeman. Maskgit: Masked generative image transformer. In *Proceedings of the IEEE/CVF Conference on Computer Vision and Pattern Recognition (CVPR)*, pages 11315–11325, June 2022.
- [3] Mark Chen, Alec Radford, Rewon Child, Jeffrey Wu, Heewoo Jun, David Luan, and Ilya Sutskever. Generative pre-training from pixels. In *International conference on machine learning*, pages 1691–1703. PMLR, 2020.
- [4] Xi Chen, Nikhil Mishra, Mostafa Rohaninejad, and Pieter Abbeel. Pixelsnail: An improved autoregressive generative model. In *International Conference on Machine Learning*, pages 864–872. PMLR, 2018.
- [5] Rewon Child, Scott Gray, Alec Radford, and Ilya Sutskever. Generating long sequences with sparse transformers. *CoRR*, abs/1904.10509, 2019.
- [6] Jacob Devlin, Ming-Wei Chang, Kenton Lee, and Kristina Toutanova. BERT: pre-training of deep bidirectional transformers for language understanding. In Jill Burstein, Christy Doran, and Thamar Solorio, editors, *Proceedings of the 2019 Conference of the North American Chapter of the Association for Computational Linguistics: Human Language Technologies, NAACL-HLT 2019, Minneapolis, MN, USA, June 2-7, 2019, Volume 1 (Long and Short Papers)*, pages 4171–4186. Association for Computational Linguistics, 2019.
- [7] Ming Ding, Zhuoyi Yang, Wenyi Hong, Wendi Zheng, Chang Zhou, Da Yin, Junyang Lin, Xu Zou, Zhou Shao, Hongxia Yang, and Jie Tang. Cogview: Mastering text-to-image generation via transformers. In Marc’Aurelio Ranzato, Alina Beygelzimer, Yann N. Dauphin, Percy Liang, and Jennifer Wortman Vaughan, editors, *Advances in Neural Information Processing Systems 34*, pages 19822–19835, 2021.
- [8] Ming Ding, Wendi Zheng, Wenyi Hong, and Jie Tang. Cogview2: Faster and better text-to-image generation via hierarchical transformers. *arXiv preprint arXiv:2204.14217*, 2022.
- [9] Alexey Dosovitskiy and Thomas Brox. Generating images with perceptual similarity metrics based on deep networks. In *Advances in Neural Information Processing Systems*, pages 658–666, 2016.
- [10] Zhengxiao Du, Yujie Qian, Xiao Liu, Ming Ding, Jiezhong Qiu, Zhilin Yang, and Jie Tang. GLM: general language model pretraining with autoregressive blank infilling. In *Proceedings of the 60th Annual Meeting of the Association for Computational Linguistics (Volume 1: Long Papers), ACL 2022, Dublin, Ireland, May 22-27, 2022*, pages 320–335. Association for Computational Linguistics, 2022.
- [11] Patrick Esser, Robin Rombach, Andreas Blattmann, and Bjorn Ommer. Imagebart: Bidirectional context with multinomial diffusion for autoregressive image synthesis. *Advances in Neural Information Processing Systems*, 34:3518–3532, 2021.
- [12] Patrick Esser, Robin Rombach, and Bjorn Ommer. Taming transformers for high-resolution image synthesis. In *Proceedings of the IEEE/CVF Conference on Computer Vision and Pattern Recognition (CVPR)*, pages 12873–12883, June 2021.
- [13] Oran Gafni, Adam Polyak, Oron Ashual, Shelly Sheynin, Devi Parikh, and Yaniv Taigman. Make-a-scene: Scene-based text-to-image generation with human priors. *arXiv preprint arXiv:2203.13131*, 2022.
- [14] Marjan Ghazvininejad, Omer Levy, Yinhan Liu, and Luke Zettlemoyer. Mask-predict: Parallel decoding of conditional masked language models. In *Proceedings of the 2019 Conference on Empirical Methods in Natural Language Processing and the 9th International Joint Conference on Natural Language Processing, EMNLP-IJCNLP 2019, Hong Kong, China, November 3-7, 2019*, pages 6111–6120. Association for Computational Linguistics, 2019.
- [15] Jiatao Gu, James Bradbury, Caiming Xiong, Victor O. K. Li, and Richard Socher. Non-autoregressive neural machine translation. In *6th International Conference on Learning Representations, ICLR 2018, Vancouver, BC, Canada, April 30 - May 3, 2018, Conference Track Proceedings*. OpenReview.net, 2018.
- [16] Shuyang Gu, Dong Chen, Jianmin Bao, Fang Wen, Bo Zhang, Dongdong Chen, Lu Yuan, and Baining Guo. Vector quantized diffusion model for text-to-image synthesis. In *IEEE/CVF Conference on Computer Vision and Pattern Recognition, CVPR 2022, New Orleans, LA, USA, June 18-24, 2022*, pages 10686–10696. IEEE, 2022.
- [17] Martin Heusel, Hubert Ramsauer, Thomas Unterthiner, Bernhard Nessler, and Sepp Hochreiter. Gans trained by a two time-scale update rule converge to a local nash equilibrium. In Isabelle Guyon, Ulrike von Luxburg, Samy Bengio, Hanna M. Wallach, Rob Fergus, S. V. N. Vishwanathan, and Roman Garnett, editors, *Advances in Neural Information Processing Systems 30: Annual Conference on Neural Information Processing Systems 2017, December 4-9, 2017, Long Beach, CA, USA*, pages 6626–6637, 2017.
- [18] Ari Holtzman, Jan Buys, Li Du, Maxwell Forbes, and Yejin Choi. The curious case of neural text degeneration. In *8th International Conference on Learning Representations, ICLR 2020, Addis Ababa, Ethiopia, April 26-30, 2020*. OpenReview.net, 2020.
- [19] Jinyi Hu, Xiaoyuan Yi, Wenhao Li, Maosong Sun, and Xing Xie. Fuse it more deeply! A variational transformer with layer-wise latent variable inference for text generation. In Marine Carpuat, Marie-Catherine de Marneffe, and Iván Vladimir Meza Ruíz, editors, *Proceedings of the 2022 Conference of the North American Chapter of the Association for Computational Linguistics: Human Language Technologies, NAACL 2022, Seattle, WA, United States, July 10-15, 2022*, pages 697–716. Association for Computational Linguistics, 2022.

- [20] Minghui Hu, Yujie Wang, Tat-Jen Cham, Jianfei Yang, and Ponnuthurai N Suganthan. Global context with discrete diffusion in vector quantised modelling for image generation. In *Proceedings of the IEEE/CVF Conference on Computer Vision and Pattern Recognition*, pages 11502–11511, 2022.
- [21] Tero Karras, Samuli Laine, and Timo Aila. A style-based generator architecture for generative adversarial networks. In *Proceedings of the IEEE/CVF conference on computer vision and pattern recognition*, pages 4401–4410, 2019.
- [22] Doyup Lee, Chihyeon Kim, Saehoon Kim, Minsu Cho, and Wook-Shin Han. Autoregressive image generation using residual quantization. In *Proceedings of the IEEE/CVF Conference on Computer Vision and Pattern Recognition (CVPR)*, pages 11523–11532, June 2022.
- [23] Junnan Li, Dongxu Li, Caiming Xiong, and Steven C. H. Hoi. BLIP: bootstrapping language-image pre-training for unified vision-language understanding and generation. In Kamalika Chaudhuri, Stefanie Jegelka, Le Song, Csaba Szepesvári, Gang Niu, and Sivan Sabato, editors, *International Conference on Machine Learning, ICML 2022, 17-23 July 2022, Baltimore, Maryland, USA*, volume 162 of *Proceedings of Machine Learning Research*, pages 12888–12900. PMLR, 2022.
- [24] Tsung-Yi Lin, Michael Maire, Serge J. Belongie, James Hays, Pietro Perona, Deva Ramanan, Piotr Dollár, and C. Lawrence Zitnick. Microsoft COCO: common objects in context. In David J. Fleet, Tomás Pajdla, Bernt Schiele, and Tinne Tuytelaars, editors, *Computer Vision - ECCV 2014 - 13th European Conference, Zurich, Switzerland, September 6-12, 2014, Proceedings, Part V*, volume 8693 of *Lecture Notes in Computer Science*, pages 740–755. Springer, 2014.
- [25] Mehdi Mirza and Simon Osindero. Conditional generative adversarial nets. *arXiv preprint arXiv:1411.1784*, 2014.
- [26] Alex Nichol, Prafulla Dhariwal, Aditya Ramesh, Pranav Shyam, Pamela Mishkin, Bob McGrew, Ilya Sutskever, and Mark Chen. Glide: Towards photorealistic image generation and editing with text-guided diffusion models. *arXiv preprint arXiv:2112.10741*, 2021.
- [27] Maria-Elena Nilsback and Andrew Zisserman. Automated flower classification over a large number of classes. In *2008 Sixth Indian Conference on Computer Vision, Graphics & Image Processing*, pages 722–729. IEEE, 2008.
- [28] Lihua Qian, Hao Zhou, Yu Bao, Mingxuan Wang, Lin Qiu, Weinan Zhang, Yong Yu, and Lei Li. Glancing transformer for non-autoregressive neural machine translation. In *Proceedings of the 59th Annual Meeting of the Association for Computational Linguistics and the 11th International Joint Conference on Natural Language Processing, ACL/IJCNLP 2021, (Volume 1: Long Papers), Virtual Event, August 1-6, 2021*, pages 1993–2003. Association for Computational Linguistics, 2021.
- [29] Alec Radford, Jong Wook Kim, Chris Hallacy, Aditya Ramesh, Gabriel Goh, Sandhini Agarwal, Girish Sastry, Amanda Askell, Pamela Mishkin, Jack Clark, Gretchen Krueger, and Ilya Sutskever. Learning transferable visual models from natural language supervision. In Marina Meila and Tong Zhang, editors, *Proceedings of the 38th International Conference on Machine Learning, ICML 2021, 18-24 July 2021, Virtual Event*, volume 139 of *Proceedings of Machine Learning Research*, pages 8748–8763. PMLR, 2021.
- [30] Samyam Rajbhandari, Jeff Rasley, Olatunji Ruwase, and Yuxiong He. Zero: memory optimizations toward training trillion parameter models. In Christine Cuiocchi, Irene Quatieri, and William T. Kramer, editors, *Proceedings of the International Conference for High Performance Computing, Networking, Storage and Analysis, SC 2020, Virtual Event / Atlanta, Georgia, USA, November 9-19, 2020*, page 20. IEEE/ACM, 2020.
- [31] Aditya Ramesh, Prafulla Dhariwal, Alex Nichol, Casey Chu, and Mark Chen. Hierarchical text-conditional image generation with clip latents. *arXiv preprint arXiv:2204.06125*, 2022.
- [32] Aditya Ramesh, Mikhail Pavlov, Gabriel Goh, Scott Gray, Chelsea Voss, Alec Radford, Mark Chen, and Ilya Sutskever. Zero-shot text-to-image generation. In *International Conference on Machine Learning*, pages 8821–8831. PMLR, 2021.
- [33] Ali Razavi, Aäron van den Oord, and Oriol Vinyals. Generating diverse high-fidelity images with VQ-VAE-2. In Hanna M. Wallach, Hugo Larochelle, Alina Beygelzimer, Florence d’Alché-Buc, Emily B. Fox, and Roman Garnett, editors, *Advances in Neural Information Processing Systems*, pages 14837–14847, 2019.
- [34] Robin Rombach, Andreas Blattmann, Dominik Lorenz, Patrick Esser, and Björn Ommer. High-resolution image synthesis with latent diffusion models. In *Proceedings of the IEEE/CVF Conference on Computer Vision and Pattern Recognition (CVPR)*, pages 10684–10695, June 2022.
- [35] Olaf Ronneberger, Philipp Fischer, and Thomas Brox. U-net: Convolutional networks for biomedical image segmentation. In *International Conference on Medical image computing and computer-assisted intervention*, pages 234–241. Springer, 2015.
- [36] Chitwan Saharia, William Chan, Saurabh Saxena, Lala Li, Jay Whang, Emily Denton, Seyed Kamyar Seyed Ghasemipour, Burcu Karagol Ayan, S. Sara Mahdavi, Rapha Gontijo Lopes, Tim Salimans, Jonathan Ho, David J. Fleet, and Mohammad Norouzi. Photorealistic text-to-image diffusion models with deep language understanding. *CoRR*, abs/2205.11487, 2022.
- [37] Tim Salimans, Ian J. Goodfellow, Wojciech Zaremba, Vicki Cheung, Alec Radford, and Xi Chen. Improved techniques for training gans. In Daniel D. Lee, Masashi Sugiyama, Ulrike von Luxburg, Isabelle Guyon, and Roman Garnett, editors, *Advances in Neural Information Processing Systems 29: Annual Conference on Neural Information Processing Systems 2016, December 5-10, 2016, Barcelona, Spain*, pages 2226–2234, 2016.
- [38] Tim Salimans, Andrej Karpathy, Xi Chen, and Diederik P Kingma. Pixelcnn++: Improving the pixelcnn with discretized logistic mixture likelihood and other modifications. *arXiv preprint arXiv:1701.05517*, 2017.
- [39] Christoph Schuhmann, Richard Vencu, Romain Beaumont, Robert Kaczmarczyk, Clayton Mullis, Aarush Katta, Theo Coombes, Jenia Jitsev, and Aran Komatsuzaki. LAION-400M: open dataset of clip-filtered 400 million image-text pairs. *CoRR*, abs/2111.02114, 2021.

- [40] Piyush Sharma, Nan Ding, Sebastian Goodman, and Radu Soricut. Conceptual captions: A cleaned, hypernymed, image alt-text dataset for automatic image captioning. In *Proceedings of the 56th Annual Meeting of the Association for Computational Linguistics (Volume 1: Long Papers)*, pages 2556–2565, Melbourne, Australia, July 2018. Association for Computational Linguistics.
- [41] Kihyuk Sohn, Honglak Lee, and Xinchen Yan. Learning structured output representation using deep conditional generative models. In Corinna Cortes, Neil D. Lawrence, Daniel D. Lee, Masashi Sugiyama, and Roman Garnett, editors, *Advances in Neural Information Processing Systems 28: Annual Conference on Neural Information Processing Systems 2015, December 7-12, 2015, Montreal, Quebec, Canada*, pages 3483–3491, 2015.
- [42] Ming Tao, Hao Tang, Songsong Wu, Nicu Sebe, Xiao-Yuan Jing, Fei Wu, and Bingkun Bao. Df-gan: Deep fusion generative adversarial networks for text-to-image synthesis. *arXiv preprint arXiv:2008.05865*, 2020.
- [43] Aaron Van den Oord, Nal Kalchbrenner, Lasse Espeholt, Oriol Vinyals, Alex Graves, et al. Conditional image generation with pixelcnn decoders. *Advances in Neural Information Processing Systems*, 29, 2016.
- [44] Aaron van den Oord, Oriol Vinyals, and koray kavukcuoglu. Neural discrete representation learning. In I. Guyon, U. Von Luxburg, S. Bengio, H. Wallach, R. Fergus, S. Vishwanathan, and R. Garnett, editors, *Advances in Neural Information Processing Systems*, volume 30. Curran Associates, Inc., 2017.
- [45] Ashish Vaswani, Noam Shazeer, Niki Parmar, Jakob Uszkoreit, Llion Jones, Aidan N Gomez, Łukasz Kaiser, and Illia Polosukhin. Attention is all you need. *Advances in Neural Information Processing Systems*, 30, 2017.
- [46] Catherine Wah, Steve Branson, Peter Welinder, Pietro Perona, and Serge Belongie. The caltech-ucsd birds-200-2011 dataset. 2011.
- [47] Ronald J. Williams and David Zipser. A learning algorithm for continually running fully recurrent neural networks. *Neural Comput.*, 1(2):270–280, 1989.
- [48] Chenfei Wu, Jian Liang, Lei Ji, Fan Yang, Yuejian Fang, Daxin Jiang, and Nan Duan. N\” uwa: Visual synthesis pre-training for neural visual world creation. *arXiv preprint arXiv:2111.12417*, 2021.
- [49] Weihao Xia, Yujiu Yang, Jing-Hao Xue, and Baoyuan Wu. Tedigan: Text-guided diverse face image generation and manipulation. In *IEEE Conference on Computer Vision and Pattern Recognition, CVPR 2021, virtual, June 19-25, 2021*, pages 2256–2265. Computer Vision Foundation / IEEE, 2021.
- [50] Tao Xu, Pengchuan Zhang, Qiuyuan Huang, Han Zhang, Zhe Gan, Xiaolei Huang, and Xiaodong He. Attngan: Fine-grained text to image generation with attentional generative adversarial networks. In *Proceedings of the IEEE conference on computer vision and pattern recognition*, pages 1316–1324, 2018.
- [51] Yu Yan, Fei Hu, Jiusheng Chen, Nikhil Bhendawade, Ting Ye, Yeyun Gong, Nan Duan, Desheng Cui, Bingyu Chi, and Ruofei Zhang. Fastseq: Make sequence generation faster. In Heng Ji, Jong C. Park, and Rui Xia, editors, *Proceedings of the Joint Conference of the 59th Annual Meeting of the Association for Computational Linguistics and the 11th International Joint Conference on Natural Language Processing, ACL 2021 - System Demonstrations, Online, August 1-6, 2021*, pages 218–226. Association for Computational Linguistics, 2021.
- [52] Jiahui Yu, Yuanzhong Xu, Jing Yu Koh, Thang Luong, Gunjan Baid, Zirui Wang, Vijay Vasudevan, Alexander Ku, Yinfei Yang, Burcu Karagol Ayan, et al. Scaling autoregressive models for content-rich text-to-image generation. *arXiv preprint arXiv:2206.10789*, 2022.
- [53] Han Zhang, Weichong Yin, Yewei Fang, Lanxin Li, Boqiang Duan, Zhihua Wu, Yu Sun, Hao Tian, Hua Wu, and Haifeng Wang. Ernie-vilg: Unified generative pre-training for bidirectional vision-language generation. *arXiv preprint arXiv:2112.15283*, 2021.
- [54] Zhu Zhang, Jianxin Ma, Chang Zhou, Rui Men, Zhikang Li, Ming Ding, Jie Tang, Jingren Zhou, and Hongxia Yang. Ufbert: Unifying multi-modal controls for conditional image synthesis. In M. Ranzato, A. Beygelzimer, Y. Dauphin, P.S. Liang, and J. Wortman Vaughan, editors, *Advances in Neural Information Processing Systems*, volume 34, pages 27196–27208. Curran Associates, Inc., 2021.
- [55] Minfeng Zhu, Pingbo Pan, Wei Chen, and Yi Yang. Dm-gan: Dynamic memory generative adversarial networks for text-to-image synthesis. In *Proceedings of the IEEE/CVF conference on computer vision and pattern recognition*, pages 5802–5810, 2019.